Published in final edited form as:
*Mol Cell Neurosci*. 2007 April ; 34(4): 539–550.

# KRIP6: a novel BTB/kelch protein regulating function of kainate receptors

**Fernanda Laezza**[*], **Timothy J Wilding**[=], **Sunitha Sequeira**[*], **Françoise Coussen**[#], **Xue Zhao Zhang**[*], **Rona Hill-Robinson**[*], **Christophe Mulle**[#], **James E Huettner**[=], and **Ann Marie Craig**[*],[1]

***** *Department of Anatomy and Neurobiology, Washington University School of Medicine, St Louis, MO 63110, USA*

= *Department of Physiology and Cell Biology, Washington University School of Medicine, St Louis, MO 63110, USA*

*# Laboratoire Physiologie Cellulaire de la Synapse, CNRS, Bordeaux Neuroscience Institute, Université Bordeaux 2, 33077 Bordeaux Cedex, France.*

## Abstract

Whereas many interacting proteins have been identified for AMPA and NMDA glutamate receptors, fewer are known to directly bind and regulate function of kainate receptors. Using a yeast two-hybrid screen for interacting partners of the C-terminal domain of GluR6a, we identified a novel neuronal protein of the BTB/kelch family, KRIP6. KRIP6 binds to the GluR6a C-terminal domain at a site distinct from the PDZ-binding motif and it co-immunoprecipitates with recombinant and endogenous GluR6. Co-expression of KRIP6 alters GluR6 mediated currents in a heterologous expression system reducing peak current amplitude and steady-state desensitization, without affecting surface levels of GluR6. Endogenous KRIP6 is widely expressed in brain and overexpression of KRIP6 reduces endogenous kainate receptor-mediated responses evoked in hippocampal neurons. Taken together, these results suggest that KRIP6 can directly regulate native kainate receptors and provide the first evidence for a BTB/kelch protein in direct functional regulation of a mammalian glutamate receptor.

### Keywords

BTB/kelch proteins; kainate receptors; GluR6; desensitization; hippocampus

## Introduction

The ionotropic glutamate receptor family includes three pharmacologically identified subtypes: NMDA (subunits NR1, NR2A–D, NR3), AMPA (GluR1–4) and kainate receptors (GluR5–7 and KA1–2) (Dingledine et al., 1999). Although the exact composition of native kainate receptors is still unclear, functional recombinant kainate receptors can be formed by homomeric channels composed of GluR5, GluR6 or GluR7, and by heteromeric combinations

Correspondence should be addressed to: Dr. Ann Marie Craig, Brain Research Centre, University of British Columbia, 2211 Wesbrook Mall, Vancouver BC, Canada V6T 2B5, Tel 604-822-7283, FAX 604-822-7299, E-mail amcraig@interchange.ubc.ca
[1]Current address: Ann Marie Craig, Brain Research Centre, University of British Columbia, 2211 Wesbrook Mall, Vancouver BC, Canada V6T 2B5

of GluR5, 6, 7 together with the KA1 or KA2 subunits (Huettner, 2003). Kainate receptors are widely expressed in the central nervous system (Wisden and Seeburg, 1993), where they can act pre- and post-synaptically. In the hippocampus, postsynaptic kainate receptors are thought to mediate excitatory transmission via an ionotropic action (Castillo et al., 1997;Cossart et al., 2002;Cossart et al., 1998) and to regulate excitability via a metabotropic function (Melyan et al., 2004;Melyan et al., 2002;Ruiz et al., 2005). Activation of presynaptic kainate receptors regulates glutamate and GABA release (Kullmann, 2001;Rodriguez-Moreno and Lerma, 1998) and modulates excitability in mature (Schmitz et al., 2000) and developing (Lauri et al., 2005) hippocampus. Kainate receptors mediate a component of synaptic transmission at mossy fiber to CA3 inputs (Castillo et al., 1997;Vignes and Collingridge, 1997) and are required for short- and long-term synaptic remodeling at hippocampal and cortical synapses (Bortolotto et al., 1999;Contractor et al., 2001;Park et al., 2006;Rodriguez-Moreno and Lerma, 1998). Kainate receptor activation contributes to developmental regulation of GABAergic transmission (Maingret et al., 2005), to seizure generation (Ben-Ari and Cossart, 2000;Mulle et al., 1998) and epileptiform burst activity (Fisahn et al., 2004).

In order to coordinate such complex functional roles, a tightly regulated mechanism must exist in neurons to target kainate receptors and regulate their functional activity. Extensive evidence demonstrates that protein-protein interactions occurring at the intracellular C-terminal domains of AMPA and NMDA receptor subunits control function and localization of these receptors (for reviews see (Bredt and Nicoll, 2003;Kim and Sheng, 2004;Song and Huganir, 2002). Synaptic insertion, recycling, and degradation of AMPA receptors is regulated by stargazin, NSF, band 4.1, and by the PDZ-domain containing proteins GRIP/ABP, PICK1, PSD-95, and SAP97. Despite the considerable information available for AMPA and NMDA receptors, less is known about proteins directly interacting with and regulating function of kainate receptors. Kainate receptors have been shown to indirectly associate with cadherin/catenin (Coussen et al., 2002), and in a more recent study to be linked to different subsets of cytosolic proteins depending on the GluR6 splice variant (Coussen et al., 2005). The majority of proteins so far identified to directly bind and regulate kainate receptors are known members of the PDZ-domain family first studied as regulators of AMPA and/or NMDA receptors. PSD-95 binds to the C-termini of GluR6 and KA2 kainate receptor subunits (Garcia et al., 1998), and GRIP and PICK1 to the C-termini of GluR6 and GluR5 (Hirbec et al., 2003), an interaction required to maintain kainate receptor synaptic function at mossy fiber to CA3 inputs (Hirbec et al., 2003).

To find new proteins directly interacting with kainate receptors, we performed a yeast two-hybrid screen of a rat brain library using the intracellular carboxyl tail of GluR6a as bait. As a result, we isolated a novel neuronal protein, which we named KRIP6 (Kainate Receptor Interacting Protein for GluR6). KRIP6 possesses a BTB/POZ (Broad-Complex, Tramtrack, and Bric-a-Brac/Poxvirus and Zincfinger) domain at the N-terminus and six kelch repeats in the C-terminal half, a typical feature of the kelch protein family. We report here that KRIP6 binds to the GluR6a C-terminal domain independently from the PDZ-domain binding site. We then show that KRIP6 interacts with GluR6 in mammalian expression systems and in brain, and that KRIP6 modulates the properties of recombinant GluR6 and of neuronal kainate receptor-mediated currents. These results define a role for a BTB/kelch protein in direct binding and regulation of a mammalian glutamate receptor and extend the class of partners directly binding to kainate receptors to a non-PDZ domain protein family.

## Results

### KRIP6 is a BTB/Kelch Protein Interacting with GluR6

To identify potential new proteins involved in the regulation of kainate receptor function, we performed a yeast-two hybrid screen of a rat forebrain cDNA library using as bait the C-

terminal domain of GluR6a (residues 842–909). We obtained two positive clones, one coding for the protein PSD-95, and the other consisting of a 540 bp cDNA fragment of unknown function. Since the interaction of GluR6 and PSD-95 was described previously (Garcia et al., 1998), we focused our studies on the novel clone. This cDNA is homologous to a clone isolated from mouse testis (accession # AK015239) and to a more recently deposited clone isolated from rat uterus (accession # NM_181473), both of unknown function. We obtained full-length cDNA by a combination of 3′ RACE and addition of synthetic 51 nt to the 5′ end corresponding to Genbank AK015239. We later named the full-length clone Kainate Receptor Interacting Protein for GluR6 (KRIP6).

KRIP6 encodes for a 600 amino acid protein with a predicted molecular mass of 68 kDa. KRIP6 possesses a BTB/POZ domain (50–163) followed by a BACK domain (167–301) and a series six of consecutive kelch repeats (314–592) (Fig. 1A; SMART analysis). The structure of KRIP6 is typical of the superfamily of kelch proteins, named after Drosophila kelch (Adams et al., 2000;Prag and Adams, 2003). Kelch superfamily proteins have diverse functions including regulating the actin cytoskeleton, gene expression, and protein ubiquitination. The BTB/POZ domain is a zinc finger and protein-protein interaction domain (Li et al., 1997) known to dimerize (e.g. (Cullen et al., 2004;Soltysik-Espanola et al., 1999). The kelch repeats, each four antiparallel β strands of 44–56 aa, combine to generate a β-propeller structure (Adams et al., 2000). The intervening BACK domain (167–301) bears homology to sequences found in BTB/kelch proteins that function as substrate-specific adaptors for protein ubiquitination (Stogios and Prive, 2004).

We performed additional yeast-two hybrid assays to test the specificity of KRIP6 interactions using the same region of KRIP6 (Fig. 1A, 18-197) that was isolated from our original yeast two hybrid screen with the GluR6a C-terminal as bait. We found no interaction of KRIP6 (18-197) with the C-terminal domains of other tested kainate receptor subunits $GluR5_{2b}$ or GluR7a (Fig. 1B). Nor did KRIP6 (18-197) interact with the C-terminal regions for AMPA receptor subunits GluR1, GluR2, or GluR3, or the NMDA receptor subunit NR2A. Thus, KRIP6 interacts selectively with the GluR6 kainate receptor subunit. We mapped the region of the GluR6a C-terminal domain required for interaction with KRIP6 and found this to be distinct from the region that interacts with PDZ domains (Fig. 1C, D). Whereas the extreme C-terminal residues of GluR6a ending in -ETMA interact with the PDZ domains of PSD-95, PICK1, and GRIP (Garcia et al., 1998;Hirbec et al., 2003), the last 10 aa were not required for interacting with KRIP6. When co-transformed with KRIP6 (18-197), the first 58 aa of the GluR6a C-terminus mediated equal β-galactosidase marker activity compared with the full 68 aa (respectively 94 ± 15 and 109 ± 15, arbitrary units, p=0.5, t-test). It is noteworthy that the C-terminal domain of GluR7a exhibits 69% identity with GluR6a over these 58 residues and yet did not bind to KRIP6 (18-197). Further studies to define the preci se interacting region of GluR6 with KRIP6 indicate it to be fairly dispersed requiring residues between 842–899 (Fig. 1C, D). Interestingly, a subsequent yeast two-hybrid screen with KRIP6 (18-197) as bait yielded a positive clone of itself. This result suggests that KRIP6 (18-197) not only binds to GluR6 but can also dimerize, similar to other BTB/kelch proteins (Adams et al., 2000).

## KRIP6 Interacts with GluR6 in Mammalian Expression Systems and In Vivo

To confirm the interaction between GluR6 and KRIP6 in a mammalian expression system, we transfected GluR6 into COS-7 cells alone or together with KRIP6 bearing an N-terminal epitope tag (Fig. 2A). COS-7 cells did not express detectable levels of endogenous KRIP6, as assayed by immunostaining or Western blot analysis using anti KRIP6#269 antibody (data not shown). We observed that, when expressed in COS-7 cells, myc-KRIP6 or CFP-KRIP6 are typically either diffuse (~60% of cells) or clustered in a perinuclear pattern (~40% of cells). On the other hand, GluR6 expressed alone in COS-7 cells shows a distribution (Fig 2A)

consistent with Golgi network and plasma membrane, as previously described (Jaskolski et al., 2004;Yan et al., 2004). When CFP-KRIP6 and GluR6 were expressed together, in 88 % of cells where CFP-KRIP6 was clustered, GluR6 assumed a clustered perinuclear pattern and co-localized with CFP-KRIP6 (Fig. 2; n=138, from 3 independent transfections). Similar results were obtained with myc-KRIP6 and GluR6 (data not shown). The change in distribution of GluR6 and the observed co-clustering with CFP-KRIP6 or myc-KRIP6 in COS-7 cells are consistent with the ability of the two proteins to interact in a mammalian expression system. To verify interaction between KRIP6 and GluR6, we expressed GluR6 alone or together with myc-KRIP6 in COS-7 cells and performed co-immunoprecipitation (Fig. 2B). The myc antibody was able to co-immunoprecipitate GluR6 only when myc-KRIP6 was co-expressed, thus confirming the interaction biochemically.

To analyze the interaction between KRIP6 and GluR6 in native tissue, we generated a rabbit polyclonal antibody against recombinant His-tagged KRIP6 (18-197). An affinity-purified fraction anti-KRIP6 # 269 was used throughout this study. This antibody recognized myc-KRIP6 by immunofluorescence (data not shown). Western blot analysis of lysate from COS-7 cells transfected with myc-KRIP6 revealed identical products of observed molecular mass of ~ 70 KD and ~ 40 kD using either anti-myc or anti-KRIP6 antibody (Fig. 2C). Such products were absent in untransfected COS-7 lysate, indicating that they both originate from myc-KRIP6 expression. The higher molecular weight band is likely to represent KRIP6 full-length product (predicted at 68 kDa), while the lower molecular weight product might result from KRIP6 degradation.

Studies of GluR6-containing complexes in native tissue have been limited by lack of appropriate antibodies against GluR6. We therefore made use of transgenic mice expressing epitope tagged myc-GluR6 in forebrain neurons; the myc-GluR6 associates with endogenous kainate receptor subunits and complements the function of native GluR6 (Coussen et al., 2002). These CaMKIIα-myc-GluR6 mice have been used to identify complexes in brain of GluR6 with cadherins/catenins and PDZ-domain proteins (Coussen et al., 2002;Hirbec et al., 2003). Western blot analysis of brain lysate of myc-GluR6 transgenic animals using anti-KRIP6 antibody revealed bands (Fig. 2D) similar to the ones we observed in transfected COS-7 cells. As shown in Fig. 2D, the anti KRIP6 antibody detected products of the same apparent molecular mass in the brain lysates from myc-GluR6 transgenic mice and in the fraction immuno-precipitated with anti-myc antibodies. These products were absent in lysates from wild type mice (Fig. 2D) immunoprecipitated using anti-myc antibodies. These results suggest that GluR6 and KRIP6 may form a complex in native tissue.

### KRIP6 Regulates Current Density and Desensitization of Recombinant GluR6

To test whether KRIP6 could affect the functional activity of GluR6 kainate receptors we analyzed whole-cell voltage clamp recordings of currents evoked by fast application of a brief pulse (~1 s) of 30 μM kainate to COS-7 cells co-transfected with untagged GluR6 and either CFP-KRIP6 or CFP empty vector. As illustrated in Fig. 3, currents mediated by GluR6 were altered by co-expression of CFP-KRIP6. First, the peak current evoked by kainate was significantly reduced in cells co-expressing CFP-KRIP6 compared to control (38.0 ± 8.9 % CFP-KRIP6 n=35 versus 100% CFP n=44, $p < 0.001$, t-test). A similar reduction in peak current amplitude was also observed for YFP-GluR6 in the presence of CFP-KRIP6 (n=8, peak reduction to 33% of control, data not shown). Secondly, co-expression of CFP-KRIP6 reduced the steady-state desensitization of GluR6 mediated currents, measured as an increase in the ratio of steady-state to peak current (378.2 ± 20.3 % n=35 compared to empty vector n=44, $p<0.001$, t-test) (Fig. 3D and 3B inset). We also evaluated the onset of desensitization of kainate evoked currents by fitting the decay time constant, Tau (Fig. 3E). We found that Tau was modestly slower in cells co-expressing CFP-KRIP6, but not statistically different from control

(p=0.23). Interestingly, the reduction in peak current and the increase in steady-state to peak level, induced by CFP-KRIP6, appeared to be two uncorrelated effects (correlation coefficients=0.096 for CFP-KRIP6; 0.203 for control), suggesting that KRIP6 either regulates GluR6 receptors via two separate mechanisms or that it acts on separate pools of GluR6 receptors. We also tested whether editing at the Q/R site of GluR6 affected the action of KRIP6 and found no difference in KRIP6 regulation between GluR6(Q) and GluR6(R) (data not shown).

The results of our yeast two-hybrid assays suggested that the kelch repeats present in full length KRIP6 were not required for interaction with the GluR6a C-terminal. To determine whether the kelch repeats were essential for physiological modulation of GluR6, we tested two additional constructs that linked CFP either to the segment of KRIP6 (1–197) that includes the BTB/POZ domain, or to the region of KRIP6 (314–600) that encodes the kelch repeats. As shown in Fig. 3G, the physiological effects of full length KRIP6 were mimicked by co-expressing the portion of KRIP6 that includes the BTB/POZ domain alone, whereas the region of KRIP6 containing only the kelch repeats had no effect. These results provide the strongest evidence that channel operation is directly regulated by binding of KRIP6 to the GluR6a C-terminal.

## KRIP6 is Widely Expressed in Brain

We next examined the endogenous distribution of KRIP6 by in situ hybridization and immunohistochemistry using coronal sections of rat brain. KRIP6 mRNA is highly expressed in 3-week postnatal rat brain, being particularly enriched in the hippocampus and in cortex (Fig. 4A). KRIP6 mRNA appears to be expressed in most neurons in these regions, matching fairly closely Nissl staining of adjacent coronal brain sections (Fig. 4, E, F, I, J). We further observed that KRIP6 mRNA expression level and distribution are developmentally regulated as indicated by comparison among 3 and 10 week old animals (Supplementary Fig. 1). Whereas at 3 weeks KRIP6 mRNA is expressed through all regions of the hippocampus and dentate gyrus, at 10 weeks it appears more segregated to the CA3 region (Supplementary Fig. 1B). This selective concentration in CA3 is remarkably similar to the distribution observed for [$^3$H] kainate binding (Foster et al., 1981;Monaghan and Cotman, 1982) and for GluR6 mRNA expression (Porter et al., 1997). We then used affinity purified anti-KRIP6 # 269 for immunohistochemical analysis on rat brain coronal sections from 3 week old animals. Consistent with the in situ hybridization data, anti-KRIP6 immunoreactivity was prominent in the cortex and in the hippocampus (Fig. 4C, G, K). KRIP6 immunoreactivity was detectable in the CA1-CA3 pyramidal cell layers of the hippocampal formation, in the granule cell layer of the dentate gyrus and in all layers (I–VI) of the cerebral cortex (Fig. 4K), similar to what was previously found for GluR6/7 immunoreactivity (Petralia et al., 1994). As revealed in high magnification images, KRIP6 immunoreactivity can be seen in the somata and in the proximal processes of neurons in the cortex and in interneurons in the hilus (Fig. 4H, L). Taken together, these results confirm the presence of KRIP6 in rat brain and reveal its expression in neurons overlapping with the distribution of GluR6.

## KRIP6 Regulates Native Kainate-Receptor Mediated Currents

We have demonstrated that KRIP6 is expressed in rat brain and that it co-immunoprecipitates with endogenous GluR6. We have also shown that KRIP6 binds to recombinant GluR6 in a heterologous expression system and profoundly alters the peak current and steady-state desensitization of GluR6 in response to fast agonist application. We therefore asked whether KRIP6 could modulate properties of native kainate receptors. To test that, whole-cell currents mediated by kainate receptors were measured in cultured hippocampal neurons transfected with CFP-KRIP6 or with CFP alone as a control. We first attempted to record spontaneous synaptic events mediated by kainate receptors to monitor potential effects of CFP-KRIP6.

However, synaptic events were not clearly detectable in our hippocampal cultures in the presence of AMPA and NMDA receptor antagonists. We then applied 300 μM kainate together with the non-competitive AMPA receptor antagonist SYM2206 (Wilding and Huettner, 2001). As shown in Fig. 5, typical kainate receptor-mediated peak currents in control cells (CFP transfected or untransfected neurons) ranged between 200 and 500 pA and showed a relatively slow onset of desensitization. However, kainate evoked smaller currents, on average, in hippocampal neurons expressing CFP-KRIP6 compared to CFP alone (54 % reduction, t-test, $p<0.05$). Native kainate receptors in cultured hippocampal neurons display less steady-state desensitization than recombinant GluR6 receptors (Wilding and Huettner, 1997) and overexpression of KRIP6 did not significantly alter desensitization of neuronal kainate receptors (Fig. 5). Our results show that elevation of KRIP6 affects currents mediated by endogenous kainate receptors in a manner similar to the action observed in the heterologous COS-7 cell expression system, effectively reducing peak currents through native kainate receptors in the hippocampal neurons. Lack of changes in desensitization might be explained if CFP-KRIP6 modulates peak current and desensitization of GluR6 containing kainate receptors via two independent mechanisms, as we postulated from our results with COS-7 cells (Fig. 3G). Alternately, the elevated steady-state to peak ratio in control neurons may preclude further regulation by addition of recombinant CFP-KRIP6. To test whether the action of CFP-KRIP6 was specific for kainate receptors, we compared currents evoked by NMDA, AMPA or GABA in control CFP versus CFP-KRIP6 expressing neurons. As shown in Fig. 6, no significant changes were found in peak current density mediated by other postsynaptic receptors. These results indicate that changes in KRIP6 levels can specifically reduce kainate receptor mediated currents in hippocampal neurons.

## KRIP6 Does Not Alter Surface Trafficking of GluR6

KRIP6 could reduce kainate receptor mediated currents by reducing the number of kainate receptors on the cell surface or by altering channel properties. In particular, given that the KRIP6 binding site (residues 842–899; Fig. 1) overlaps an identified forward trafficking determinant in GluR6 (residues 872–880; (Jaskolski et al., 2004;Yan et al., 2004), it seemed a likely possibility that KRIP6 might alter surface trafficking of GluR6. To test this idea, we determined whether KRIP6 changes surface levels of co-expressed GluR6 in both COS-7 cells and in hippocampal neurons. Since antibodies against the native GluR6 extracellular domain were not available for live cell imaging, we expressed a form of GluR6 bearing an extracellular YFP tag (modified from GFP-GluR6 of (Yan et al., 2004). YFP-GluR6 was co-expressed with CFP-KRIP6 or with CFP as control, and the YFP-GluR6 surface pool was labeled using an antibody against YFP applied live, followed by application of a secondary antibody after fixation. There was no obvious difference in the surface labeling pattern or intensity of YFP-GluR6 in COS-7 cells expressing CFP-KRIP6 versus CFP (Fig. 7A). In some CFP-KRIP6-expressing cells, the pattern of total cellular YFP-GluR6 was similar to control (as in Fig. 7A), while in others the YFP-GluR6 was present in coclusters with KRIP6 (like Fig. 1A), but these co-clusters generally did not label for surface anti-YFP and thus are mainly intracellular. Moreover, quantitation of a random population of cells (including both clustered and diffuse patterns) revealed no difference in immunofluorescence intensity of surface labeled YFP-GluR6 in cells coexpressing CFP-KRIP6 compared with CFP. This was true whether surface YFP-GluR6 measures were compared as absolute intensity (Fig. 7B; 84 ± 13 % compared to control, $n=24$, $p>0.1$ unpaired t-test) or normalized to total YFP-GluR6 intensity per cell (data not shown), indicating that KRIP6 does not affect GluR6 surface trafficking. The total level of YFP-GluR6 was also unchanged by the presence of CFP-KRIP6, indicating that CFP-KRIP6 is not affecting expression level or degradation of YFP-GluR6. Thus changes in GluR6 mediated currents observed in the presence of CFP-KRIP6 are likely to result from modulation of channel properties in COS-7 cells.

We repeated essentially the same experiments in hippocampal neurons and again found that co-expression of CFP-KRIP6 did not alter surface levels of YFP-GluR6 in hippocampal neurons (Fig. 7B, C). In these neurons, total and surface YFP-GluR6 was largely somatodendritic, co-localizing with the dendritic marker MAP2, and not readily detectable in axons (Fig. 7C). This distribution is similar to the pattern we observed for endogenous GluR6/7 using an antibody against an intracellular determinant (data not shown). Co-expression of CFP-KRIP6 did not obviously alter the polarized distribution or surface levels of YFP-GluR6, an impression confirmed by quantitative analysis (Fig. 7B; 90 ± 4 % compared to control, n=52, $p>0.1$ unpaired t-test). These studies suggest that KRIP6 does not alter kainate receptor surface trafficking in neurons, but most likely it acts by modulating channel properties as in COS-7 cells.

## Discussion

We have identified a novel neuronal BTB/kelch superfamily protein, KRIP6, which binds to and regulates the function of GluR6-containing kainate receptors. KRIP6 is widely expressed and developmentally regulated in brain where it forms a complex with GluR6. KRIP6 binds to the GluR6a C-terminal domain at a site independent from a previously identified PDZ-domain binding site. When co-expressed with recombinant GluR6 in mammalian cells, KRIP6 and GluR6 co-cluster and KRIP6 reduces peak current and steady-state desensitization by an effect on channel properties rather than trafficking. Overexpression of KRIP6 in hippocampal neurons reduces peak current mediated by native kainate receptors, leaving AMPA, NMDA and GABA receptor-mediated responses unchanged. KRIP6 is widely expressed and developmentally regulated in brain. Taken together, these results provide evidence for functional regulation of native kainate receptor mediated responses by a newly identified neuronal protein of the BTB/kelch family.

KRIP6 belongs to the superfamily of BTB/kelch proteins, as indicated by the presence of a BTB/POZ domain and a series of kelch repeats (Adams et al., 2000;Prag and Adams, 2003). BTB/kelch proteins are highly conserved across species, yet their functional roles appear quite diverse, ranging from organization of cytoskeletal elements to control of protein trafficking/ubiquitination and regulation of gene expression. Two brain-enriched BTB/kelch proteins closely related to KRIP6, Mayven and actinfilin, associate with the actin cytoskeleton (Chen et al., 2002;Soltysik-Espanola et al., 1999). However, unlike Mayven and actinfilin, KRIP6 does not colocalize with F-actin in COS-7 cells or in neurons, and thus probably does not bind actin. Based on yeast two-hybrid studies and on physiological recordings with separate N-terminal and C-terminal domain constructs, we conclude that the interaction between KRIP6 and kainate receptors likely involves the BTB/POZ domain located within the N-terminal region of KRIP6. Consistent with other BTB/kelch family members, in which BTB/POZ domains mediate both homophilic and heterophilic interactions, the segment of KRIP6 that includes the BTB/POZ domain appears to bind to itself as well as to a domain within the first 58 amino acids of the GluR6a cytoplasmic C-terminus. Interestingly, the binding of KRIP6 to GluR6a does not require the final 10 amino acids of the GluR6 C-terminus, which include the -ETMA motif that is essential for interactions with PDZ domain-containing proteins such as PSD-95 and PICK1.

Kainate receptors function as homomeric or heteromeric combinations of four individual subunits, which form a conducting pathway through the membrane similar in structure to the KcsA potassium channel, but with inverted topology. Agonist binding to these receptors induces a series of conformational changes, such that channels initially open and then subsequently desensitize. Our physiological experiments indicate that KRIP6 regulates functional aspects of both native and recombinant kainate receptors. Overexpression of KRIP6 in hippocampal neurons reduces peak current amplitude mediated by native kainate receptors,

leaving AMPA, NMDA and GABA receptor-mediated currents unchanged. In transfected COS-7 cells, co-expression of KRIP6 caused a similar reduction of peak current amplitude mediated by homomeric GluR6 receptors, and also decreased the level of steady-state desensitization. The physiological effects of KRIP6 were not accompanied by any significant change in recombinant receptor surface levels in COS-7 cells or in neurons, suggesting a direct effect on channel gating or conductance rather than a change in receptor trafficking. Moreover, the fact that similar changes in GluR6-mediated currents were observed upon co-expression of the truncated KRIP6 (18-197) construct suggests that kainate receptor modulation described in this study results directly from KRIP6 binding, and does not require possible downstream interactions involving the kelch repeats.

The two effects of KRIP6 on recombinant receptor physiology were not strongly correlated. Some KRIP6-expressing cells exhibited small peak currents and large steady-state/peak ratios; however, many other cells exhibited relatively small peak currents with steady-state desensitization comparable to control cells. In addition, a few cells displayed reduced desensitization but relatively large peak currents. Collectively, these results suggest that KRIP6 exerts an independent action on peak current amplitude and steady-state desensitization. This interpretation is consistent with previous evidence for both kainate (Bowie and Lang, 2002) and AMPA (Tang et al. 1989;Bowie and Lange, 2002) receptors that different open states underlie the initial peak current and the steady-state current recorded at equilibrium. In addition, the independent effects of KRIP6 on peak and steady-state currents may reflect differences among channel populations in the phosphorylation (Raymond et al., 1993;Wang et al., 1993) or palmitoylation (Pickering et al., 1995) state of GluR6. Such post-translational modifications could functionally segregate GluR6 containing kainate receptors into different pools or vary accessibility to functional regulation by KRIP6. Our experiments also revealed no significant difference in the time constant of desensitization (Tau) between control cells and those co-expressing full length KRIP6. This result agrees with an earlier study (Bowie et al. 2003) of channel regulation that used high speed agonist applications to outside-out macropatches. Bowie and colleagues (2003) found no change in the time constant of desensitization following modulation of homomeric GluR6 channels by extracellular treatment with Con A (Huettner, 1990), or by co-expression of the cytoplasmic PDZ domain protein PSD-95 (Garcia et al., 1998).

Native kainate receptors in hippocampal neurons are likely to be heteromeric assemblies of GluR6 with other subunits. Cultured neurons of the type recorded here express high levels of GluR6 and KA2, and more variable levels of GluR5 and GluR7 (Craig et al., 1993;Roche and Huganir, 1995). Thus, although the exact stoichiometry is not known, kainate currents in the hippocampal neuron preparation used in this study are likely mediated by receptors containing from 1 to 3 GluR6 subunits, and thus from 1 to 3 KRIP6 binding sites. In contrast, homomeric receptors expressed in GluR6-transfected COS-7 cells would include 4 GluR6 subunits, each with the potential to bind KRIP6. These differences in subunit composition are likely to underlie the distinct kinetics of native receptors versus homomeric recombinant channels formed by GluR6 alone. Subunit composition might also explain the lack of effect of KRIP6 on the steady-state to peak ratio in neurons, although we cannot rule out potential interference or interaction with other endogenous neuronal proteins that might influence the accessibility of the target domain(s) bound by KRIP6.

Given their independent binding sites, there is potential for GluR6 to bind to both KRIP6 and PDZ domain proteins. By delivery of peptides designed to interfere with binding of $GluR5_{(2b\ and\ 2c)}$ and GluR6 to GRIP and PICK1, Hirbec et al. (2003) reported a role for these interactions in maintaining kainate receptor-mediated synaptic function at hippocampal mossy fiber-CA3 synapses. In contrast, we find that KRIP6 acts to reduce kainate receptor-mediated peak currents in hippocampal neurons. The PDZ domain proteins PSD-95 and syntenin also

bind GluR5 and GluR6 and may modulate receptor function (Bowie et al., 2003;Garcia et al., 1998;Hirbec et al., 2003). KRIP6 differs from these other kainate receptor interacting proteins in that it binds the C-terminal domain of GluR6 but not other kainate, AMPA, or NMDA receptor subunits tested, and thus may function more specifically to regulate only GluR6-containing kainate receptors.

KRIP6 is widely expressed in brain, as shown by in situ hybridization and immunohistochemistry, with high levels of expression in cortex and hippocampus where expression of GluR6 is also prominent (Petralia et al., 1994;Porter et al., 1997). KRIP6 co-clusters and co-imunoprecipitates with recombinant GluR6 in a heterologous mammalian expression system and co-immunoprecipitates with endogenous GluR6 in brain homogenates. Changes in the levels and distribution of KRIP6 occur developmentally in the hippocampus (Supplementary Fig. 1), suggesting that KRIP6 expression is under dynamic control. Fine changes in the level of KRIP6 could have important consequences for neurons, modulating kainate-receptor mediated responses. High levels of KRIP6 might protect neurons during high frequency release of glutamate by inhibiting kainate receptor-mediated peak current, reducing postsynaptic depolarization and excessive divalent influx. High levels of KRIP6 might also favor elevated steady-state kainate responses, increasing input temporal summation (Frerking and Ohliger-Frerking, 2002) or affect kainate-induced gamma oscillations and epileptiform bursts (Fisahn et al., 2004).

## Experimental Methods

### Yeast two-hybrid screening

We used as bait the whole GluR6a C-terminal domain (aa 842–909) subcloned into ppC97, which contains the GAL4 DNA binding domain. A random-primed library from rat cortex and hippocampus cloned into ppC86, which contains the GAL4 activation domain, was kindly provided by Dr. P. Worley (Johns Hopkins University). Glutamate receptor cDNAs were a gift of Dr. J. Boulter (UCLA). The bait was cotransformed with the library in the yeast strain PJ69-4A harboring HIS3, ADE2, and lacZ reporter genes (James et al., 1996). Positive clones were selected on plates lacking leucine, tryptophan and histidine. The positive clones were further selected by growing in a medium lacking leucine, tryptophan, histidine, and adenine and then were tested for beta-galactosidase activity (Yeast beta-Galactosidase Assay Kit, Pierce). The positive clones were rescued, retransformed to confirm the interaction, and sequenced. For further yeast-two hybrid assays, KRIP6 (18-197) was subcloned in ppC86. Interaction of KRIP6 with the C-terminal domains of other glutamate receptors and truncation constructs of GluR6 subcloned in ppC97 were then tested as listed in Fig. 1B, C. All constructs were generated by PCR or by site directed mutagenesis (Quick Change XL, Stratagene) to introduce a premature STOP codon, and verified by sequencing.

### Cloning of KRIP6 cDNA

We obtained the 3′ end of the KRIP6 coding region by nested PCR amplification of rat brain cDNA (Marathon RACE, Clontech). The cDNAs contain overlapping adaptors at both 5′ and 3′ ends, AP1 and AP2. Cloning was performed using three consecutive PCR cycles with the following primer pairs: CAGCCTGTAGCAGCTACTTCAGAGCCAT (236–263) and AP1; then GAGGAGCAGCTTGATCCTTGCAACTGCT (460–493) and AP2; then CCAGCGTTTCGCCGACACCCACTCACTC (496–522) and AP2. The final PCR reaction produced a single band of ~1.4 kb that was ligated into pGEM T/A vector and confirmed by sequencing. The full coding region of KRIP6 was then reconstituted from the yeast two-hybrid clone, the 3′ RACE product, and a custom synthesized 51 nt to complete the 5′ end. The 51 nt added to complete the 5′ coding sequence were derived from Genbank AK015239 and

correspond to the start site that is conserved between mouse, rat, and human clones, excluding the additional possible 5′ coding sequence present only in the mouse cDNA.

### Antibody generation and purification

KRIP6 (18-197) was subcloned into vector p-ET-28c (Novagen) in a fusion with N-terminal and C-terminal polyhistidine ($His_6$) tags and transformed into E. coli BL21. Following induction of the fusion protein (100 μM IPTG for 2 hours at 37 C), the $His_6$ –tagged fusion protein was isolated from inclusion bodies and column purified using His Bind purification kit (Novagen). The fusion protein was run on an acrylamide gel (12%), visualized with Coomassie staining, gel extracted and used as immunogen. Two rabbits (#268 and #269) were immunized by Covance Research Products. Antiserum from rabbit #269 was subjected to Protein A-column purification followed by affinity purification on $His_6$-KRIP6 (18-197) cross-linked to Affigel-10 (BioRad) and used for this study.

### Cell culture, transfection, and immunocytochemistry

Rat hippocampal cultures were prepared from E-18 rat embryos by previously described methods (Goslin et al., 1998). Neurons were maintained on polylysine-coated glass coverslips suspended above a glial feeder layer, in serum-free N2.1 media containing 100 μM APV. COS-7 cells were obtained from ATCC and maintained in DMEM and 10 % FBS. All transfections were done using Lipofectamine 2000 (Invitrogen). Neurons were transfected at 12 days in vitro (DIV) and analyzed at 14 DIV. GluR6a (Q) cDNA was expressed from the pEYFP-N1 expression vector (Clontech), either untagged or N-terminally YFP tagged. N-terminally epitope-tagged forms of KRIP6 were expressed from myc-pRK5 (obtained from P. Worley) and from pECFP-N1 (Clontech).

**Surface receptor—**Neurons or COS-7 cells were incubated 15 min at room temperature in primary antibody (Ab) diluted in respectively N2.1 or COS-7 media with the addition of HEPES buffer (50 μM; pH 7.4). Cells were rinsed using fresh media with HEPES buffer, and then fixed in 4 % paraformaldehyde (PFA) and 4% sucrose.

**Immunostaining—**Following fixation, cells were permeabilized in 0.25% Triton X-100, incubated in 10% BSA for 30 min at 37°C to block nonspecific staining and incubated in appropriate primary Ab (overnight at room temperature). After washing in PBS, cells were incubated in secondary Ab (45 min; 37°C). The coverslips were mounted in elvanol (Tris-HCl, glycerol, and polyvinyl alcohol with 2% 1,4-diazabicyclo [2,2,2] octane).

**Antibodies—**Primary antibodies were: rabbit anti-GFP for COS cells (1:1000, Molecular Probes); Texas Red-conjugated anti-GFP for neurons (1:2000, Roche); rabbit anti-GluR6/7 (1:600, Upstate), mouse anti-myc (1:1000, 9E10 clone, Upstate), mouse anti-MAP2 (1:2000, Chemicon). Secondary antibodies were: Alexa 568 anti-mouse IgG1 (1:500), Alexa 647 anti-rabbit or anti-mouse (1:500) (all from Molecular Probes).

### Image analysis

All fluorescence and phase contrast images were acquired with a Photometrics Sensys cooled CCD camera on a Axioskop microscope (Zeiss) with a 63X (for COS-7 cells) or 40X (for neurons) objective, using Metamorph software (Universal Imaging). Sets of cells compared for quantitation were stained simultaneously and chosen randomly based only on expression of the transfected protein and healthy morphology. Images were randomized for blind quantitation. The area of analysis for each cell was defined by CFP or CFP-KRIP6 cell fill for COS-7 cells or by MAP2 immunofluorescence for neurons. Analysis was performed using

Metamorph and Microsoft Excel. All statistical comparisons of immunofluorescence were made using Student's *t* test. Images were prepared for printing using Adobe Photoshop.

## Immunoprecipitation and Western blot

**Heterologous cells—**COS-7 cells were transfected with myc-KRIP6 and GluR6 for co-immunoprecipitation in heterologous cells. At 48 h post-transfection, the cells were washed twice with phosphate-buffered saline and scraped in 800 μl of RIPA buffer [50 mM Tris-HCl (pH 7.4), 1% Triton X-100, 0.5 % Na-deoxycholate, 0.15 M NaCl, 1 mM EDTA, and a protease inhibitor mixture (Calbiochem, protease inhibitor set # 3, 1:100)]. After sonication, the supernatant was centrifuged at maximum speed on a table top centrifuge at 4°C for 15 min. The supernatant was then incubated with the corresponding antibody for 3.5 hr and then 20 μl of protein G-Sepharose (1:1 slurry) was added to the complex for 2.5 hr at 4°C. The mixture was washed three times with RIPA buffer, one time with 150 mM NaCl and two times with RIPA buffer. The proteins were eluted with 20 μl 2X Laemmli Buffer. Mixtures were heated for 15 min at 70°C and loaded on a 4–15% polyacrylamide gel (BioRad). Resolved proteins were transferred to PVDF membranes (Millipore) overnight at 4°C and blocked in Tris-buffered saline (TBS) with 5% skim milk and 0.1% Tween-20. Membranes were then incubated in blocking buffer containing rabbit anti-GluR6/7 antibody (1:5000, Upstate), monoclonal anti-Myc (1:5000, Upstate), or rabbit anti-KRIP6 (1: 2000). Washed membranes were incubated with HRP conjugated secondary antibodies and detected with SuperSignal Pico chemiluminescent substrate (Pierce).

**Brain—**Membrane fractions from wild type C57BL/6 or CaMKIIα-myc-GluR6 mouse brain were collected and solubilized in a buffer containing 20 mM HEPES, 1% Triton X-100, 150 mM NaCl, 0.15 mM EDTA and anti-protease cocktail as described (Coussen et al., 2002). Solubilized brain membrane lysate (1.5 ml) was incubated with 30 μl of magnetic protein G beads (Miltenyi Biotec) for 40 min at 4°C and centrifuged. The cleared supernatant was incubated with anti-myc antibody for 1 hr at 4°C and then overnight with 30 μl of magnetic protein G beads at 4°C. Immunoprecipitated proteins were eluted with 100 μl of SDS sample buffer (50 mM Tris-HCl, pH 6.8, 2% SDS, 10% glycerol, 100 mM DTT and bromophenol blue) for immunoblotting with the anti-KRIP6 antibody.

## In situ hybridization

Digoxigenin-labeled RNA probes were prepared by subcloning KRIP6 nt 52–592 into pGEM vector and transcription with T7 (anti-sense probe) or SP6 (sense control probe) RNA polymerase (DIG RNA Labeling Kit, Roche). Purity of the probes was assessed by gel electrophoresis and the efficiency of the transcription reaction was checked using dot blot analysis. Brains were dissected from 3 or 10 weeks old male Sprague-Dawley rats after anesthetization and perfusion with 4% PFA. After rinsing in PBS, free-floating sections (30 μm) were treated with 10 μg/ml proteinase K (Invitrogen) at 37°C and acetylated in 0.25% acetic anhydride in 0.1 M triethanolamine for 10 min. Coronal sections were rinsed in 2X SSC (20X SSC = 3M NaCl, 0.3M NaCitrate, pH 7.0) for 5 min. After prehybridization for 1h at 55° C in hybridization buffer (50% formamide, 4XSSC, 1X Denhardt's solution, 10% dextran sulfate, 0.25 mg/ml yeast tRNA, 0.5 mg/ml salmon sperm DNA), hybridization was performed overnight at 55 °C in hybridization buffer plus 300 ng/ml digoxigenin-labeled cRNA KRIP6 probe. Sections were washed in 0.2X SSC at 55°C 20 min 3 times and washed with 2X SSC, 1X SSC, 0.5X SSC each 10 min at room temperature. Hybridized digoxigenin-labeled RNA was detected with alkaline phosphatase-linked anti-digoxigenin Fab fragments (Roche) followed by a reaction with NBT/BCIP. Sections were mounted in Crystal/Mount (Biomeda Corporation).

### Immunohistochemistry

Brain sections that were prepared for in situ hybridization were processed in parallel for immunohistochemistry following 4 % PFA fixation. Staining was performed either on free floating sections or on brain slices dessicated on glass slides. Slices were treated with 0.3 % $H_2O_2$ for 20–30 min to quench endogenous peroxidase activity, permeabilized with 0.5 % Triton X-100 for 15–20 min, and blocked with 10% NGS for 45 min. Sections were incubated at room temperature overnight with affinity purified anti-KRIP6 or preimmune IgG fraction in PBS + 3 % BSA. The sections were incubated with 1:300 biotinylated goat anti-rabbit antibody in PBS for 1 hr, and subsequently incubated with Vectastain Elite ABC kit reagents (Vector Labs, CA) for 30 min to allow formation of avidin-biotin complexes. Colorimetric reaction was obtained using a 3,3-diaminobenzidine tetrahydrochloride (DAB) and nickel solution reaction (DAB substrate kit, Vector Labs, CA). The sections were then dehydrated and mounted.

### Electrophysiology

Cultures were perfused at 1 to 2 ml/min with Tyrode's solution (in mM): 150 NaCl, 4 KCl, 2 $CaCl_2$, 2 $MgCl_2$, 10 glucose, 10 HEPES, pH adjusted to 7.4 with NaOH. Whole-cell electrodes were filled with (in mM) 140 Cs-glucuronate, 10 CsCl, 10 $MgCl_2$, 10 EGTA, 5 ATP, 1 GTP, 10 HEPES, pH adjusted to 7.4 with CsOH. The open tip resistance was typically 1 to 5 MΩ. The reference electrode was in a well filled with internal solution that connected to the bath via an agar bridge equilbrated with 4 M KCl. Currents were recorded with an Axopatch 200 A amplifier, filtered at 1 kHz and digitized at 10 kHz. Cells were held at −70 to −80 mV.

**Drug Applications—**A multibarreled local perfusion pipette was used to apply control and kainate-containing solutions to cells under whole-cell clamp. Kainate was dissolved at 300 μM in a control extracellular solution consisting of (in mM): 160 NaCl, 10 HEPES, 2 $CaCl_2$, pH adjusted to 7.4 with NaOH. For rapid applications, the drug reservoirs were held under static air pressure (5 to 10 psi) and solution flow was controlled by computer-gated electronic valves (The Lee Co.). The time constant for solution exchange during whole-cell recordings was 5 to 15 msec. Although faster solution changes can be achieved with outside-out patch recordings, allowing for optimal kinetic measurements, the fact that each patch samples a different fraction of the total surface channel population precludes meaningful comparison of peak current amplitude from one patch to the next. By contrast, whole-cell experiments record current through all of the functional channels present on the cell surface. For this study, whole-cell recordings were used to allow simultaneous comparison of relative peak and steady-state levels between control and KRIP6-transfected cells. Results are presented as mean ± SEM.

## Supplementary Material

Refer to Web version on PubMed Central for supplementary material.

#### Acknowledgements

We thank Huaiyang Wu for excellent preparation of neuron cultures, Drs. Paul Worley and Anthony Lanahan for the gift of the yeast two-hybrid library, and Dr. Anis Contractor for the EGFP-GluR6 construct. This work was supported by the AES fellowship provided by the Milken Family Foundation (FL), Washington University Young Scientist Program (RHR), NIH and NIH NS39286 (AMC).

## References

Adams J, Kelso R, Cooley L. The kelch repeat superfamily of proteins: propellers of cell function. Trends Cell Biol 2000;10:17–24. [PubMed: 10603472]

Ben-Ari Y, Cossart R. Kainate, a double agent that generates seizures: two decades of progress. Trends Neurosci 2000;23:580–587. [PubMed: 11074268]

Bortolotto ZA, Clarke VR, Delany CM, Parry MC, Smolders I, Vignes M, Ho KH, Miu P, Brinton BT, Fantaske R, et al. Kainate receptors are involved in synaptic. plasticity. Nature 1999;402:297–301. [PubMed: 10580501]

Bowie D, Lange GD. Functional stoichiometry of glutamate receptor desensitization. J Neurosci 2002;22:3392–3403. [PubMed: 11978816]

Bowie D, Garcia EP, Marshall J, Traynelis SF, Lange GD. Allosteric regulation and spatial distribution of kainate receptors bound to ancillary proteins. J Physiol 2003;547:373–385. [PubMed: 12562952]

Bredt DS, Nicoll RA. AMPA receptor trafficking at excitatory synapses. Neuron 2003;40:361–379. [PubMed: 14556714]

Castillo PE, Malenka RC, Nicoll RA. Kainate receptors mediate a slow postsynaptic current in hippocampal CA3 neurons. Nature 1997;388:182–186. [PubMed: 9217159]

Chen Y, Derin R, Petralia RS, Li M. Actinfilin, a brain-specific actin-binding protein in postsynaptic density. J Biol Chem 2002;277:30495–30501. [PubMed: 12063253]

Contractor A, Swanson G, Heinemann SF. Kainate receptors are involved in short- and long-term plasticity at mossy fiber synapses in the hippocampus. Neuron 2001;29:209–216. [PubMed: 11182092]

Cossart R, Epsztein J, Tyzio R, Becq H, Hirsch J, Ben-Ari Y, Crepel V. Quantal release of glutamate generates pure kainate and mixed AMPA/kainate EPSCs in hippocampal neurons. Neuron 2002;35:147–159. [PubMed: 12123615]

Cossart R, Esclapez M, Hirsch JC, Bernard C, Ben-Ari Y. GluR5 kainate receptor activation in interneurons increases tonic inhibition of pyramidal cells. Nat Neurosci 1998;1:470–478. [PubMed: 10196544]

Coussen F, Normand E, Marchal C, Costet P, Choquet D, Lambert M, Mege RM, Mulle C. Recruitment of the kainate receptor subunit glutamate receptor 6 by cadherin/catenin complexes. J Neurosci 2002;22:6426–6436. [PubMed: 12151522]

Coussen F, Perrais D, Jaskolski F, Sachidhanandam S, Normand E, Bockaert J, Marin P, Mulle C. Co-assembly of two GluR6 kainate receptor splice variants within a functional protein complex. Neuron 2005;47:555–566. [PubMed: 16102538]

Craig AM, Blackstone CD, Huganir RL, Banker G. The distribution of glutamate receptors in cultured rat hippocampal neurons: postsynaptic clustering of AMPA-selective subunits. Neuron 1993;10:1055–1068. [PubMed: 7686378]

Cullen VC, Brownlees J, Banner S, Anderton BH, Leigh PN, Shaw CE, Miller CC. Gigaxonin is associated with the Golgi and dimerises via its BTB domain. Neuroreport 2004;15:873–876. [PubMed: 15073534]

Dingledine R, Borges K, Bowie D, Traynelis SF. The glutamate receptor ion channels. Pharmacol Rev 1999;51:7–61. [PubMed: 10049997]

Fisahn A, Contractor A, Traub RD, Buhl EH, Heinemann SF, McBain CJ. Distinct roles for the kainate receptor subunits GluR5 and GluR6 in kainate-induced hippocampal gamma oscillations. J Neurosci 2004;24:9658–9668. [PubMed: 15509753]

Foster AC, Mena EE, Monaghan DT, Cotman CW. Synaptic localization of kainic acid binding sites. Nature 1981;289:73–75. [PubMed: 6256647]

Frerking M, Ohliger-Frerking P. AMPA receptors and kainate receptors encode different features of afferent activity. J Neurosci 2002;22:7434–7443. [PubMed: 12196565]

Garcia EP, Mehta S, Blair LA, Wells DG, Shang J, Fukushima T, Fallon JR, Garner CC, Marshall J. SAP90 binds and clusters kainate receptors causing incomplete desensitization. Neuron 1998;21:727–739. [PubMed: 9808460]

Goslin, K.; Asmussen, H.; Banker, G. Rat hippocampal neurons in low-density culture. In: Banker, G.; Goslin, K., editors. Culturing Nerve Cells. Cambridge: MIT Press; 1998. p. 339-370.

Hirbec H, Francis JC, Lauri SE, Braithwaite SP, Coussen F, Mulle C, Dev KK, Coutinho V, Meyer G, Isaac JT, et al. Rapid and differential regulation of AMPA and kainate receptors at hippocampal mossy fibre synapses by PICK1 and GRIP. Neuron 2003;37:625–638. [PubMed: 12597860]

Huettner JE. Glutamate receptor channels in rat DRG neurons. Activation by kainate and quisqualate, and blockade of desensitization by Con A. Neuron 1990;5:255–266. [PubMed: 2169266]

Huettner JE. Kainate receptors and synaptic transmission. Prog Neurobiol 2003;70:387–407. [PubMed: 14511698]

James P, Halladay J, Craig EA. Genomic libraries and a host strain designed for highly efficient two-hybrid selection in yeast. Genetics 1996;144:1425–1436. [PubMed: 8978031]

Jaskolski F, Coussen F, Nagarajan N, Normand E, Rosenmund C, Mulle C. Subunit composition and alternative splicing regulate membrane delivery of kainate receptors. J Neurosci 2004;24:2506–2515. [PubMed: 15014126]

Kim E, Sheng M. PDZ domain proteins of synapses. Nat Rev Neurosci 2004;5:771–781. [PubMed: 15378037]

Kullmann DM. Presynaptic kainate receptors in the hippocampus: slowly emerging from obscurity. Neuron 2001;32:561–564. [PubMed: 11719198]

Lauri SE, Segerstrale M, Vesikansa A, Maingret F, Mulle C, Collingridge GL, Isaac JT, Taira T. Endogenous activation of kainate receptors regulates glutamate release and network activity in the developing hippocampus. J Neurosci 2005;25:4473–4484. [PubMed: 15872094]

Li X, Lopez-Guisa JM, Ninan N, Weiner EJ, Rauscher FJ 3rd, Marmorstein R. Overexpression, purification, characterization, and crystallization of the BTB/POZ domain from the PLZF oncoprotein. J Biol Chem 1997;272:27324–27329. [PubMed: 9341182]

Maingret F, Lauri SE, Taira T, Isaac JT. Profound regulation of neonatal CA1 rat hippocampal GABAergic transmission by functionally distinct kainate receptor populations. J Physiol 2005;567:131–142. [PubMed: 15946969]

Melyan Z, Lancaster B, Wheal HV. Metabotropic regulation of intrinsic excitability by synaptic activation of kainate receptors. J Neurosci 2004;24:4530–4534. [PubMed: 15140923]

Melyan Z, Wheal HV, Lancaster B. Metabotropic-mediated kainate receptor regulation of IsAHP and excitability in pyramidal cells. Neuron 2002;34:107–114. [PubMed: 11931745]

Monaghan DT, Cotman CW. The distribution of [3H]kainic acid binding sites in rat CNS as determined by autoradiography. Brain Res 1982;252:91–100. [PubMed: 6293660]

Mulle C, Sailer A, Perez-Otano I, Dickinson-Anson H, Castillo PE, Bureau I, Maron C, Gage FH, Mann JR, Bettler B, Heinemann SF. Altered synaptic physiology and reduced susceptibility to kainate-induced seizures in GluR6-deficient mice. Nature 1998;392:601–605. [PubMed: 9580260]

Park Y, Jo J, Isaac JT, Cho K. Long-term depression of kainate receptor-mediated synaptic transmission. Neuron 2006;49:95–106. [PubMed: 16387642]

Petralia RS, Wang YX, Wenthold RJ. Histological and ultrastructural localization of the kainate receptor subunits, KA2 and GluR6/7, in the rat nervous system using selective antipeptide antibodies. J Comp Neurol 1994;349:85–110. [PubMed: 7852627]

Pickering DS, Taverna FA, Salter MW, Hampson DR. Palmitoylation of the GluR6 kainate receptor. Proc Natl Acad Sci U S A 1995;92:12090–12094. [PubMed: 8618850]

Porter RH, Eastwood SL, Harrison PJ. Distribution of kainate receptor subunit mRNAs in human hippocampus, neocortex and cerebellum, and bilateral reduction of hippocampal GluR6 and KA2 transcripts in schizophrenia. Brain Res 1997;751:217–231. [PubMed: 9099808]

Prag S, Adams JC. Molecular phylogeny of the kelch-repeat superfamily reveals an expansion of BTB/kelch proteins in animals. BMC Bioinformatics 2003;4:42. [PubMed: 13678422]

Raymond LA, Blackstone CD, Huganir RL. Phosphorylation and modulation of recombinant GluR6 glutamate receptors by cAMP-dependent protein kinase. Nature 1993;361:637–641. [PubMed: 8094892]

Roche KW, Huganir RL. Synaptic expression of the high-affinity kainate receptor subunit KA2 in hippocampal cultures. Neuroscience 1995;69:383–393. [PubMed: 8552236]

Rodriguez-Moreno A, Lerma J. Kainate receptor modulation of GABA release involves a metabotropic function. Neuron 1998;20:1211–1218. [PubMed: 9655508]

Ruiz A, Sachidhanandam S, Utvik JK, Coussen F, Mulle C. Distinct subunits in heteromeric kainate receptors mediate ionotropic and metabotropic function at hippocampal mossy fiber synapses. J Neurosci 2005;25:11710–11718. [PubMed: 16354929]

Schmitz D, Frerking M, Nicoll RA. Synaptic activation of presynaptic kainate receptors on hippocampal mossy fiber synapses. Neuron 2000;27:327–338. [PubMed: 10985352]

Soltysik-Espanola M, Rogers RA, Jiang S, Kim TA, Gaedigk R, White RA, Avraham H, Avraham S. Characterization of Mayven, a novel actin-binding protein predominantly expressed in brain. Mol Biol Cell 1999;10:2361–2375. [PubMed: 10397770]

Song I, Huganir RL. Regulation of AMPA receptors during synaptic plasticity. Trends Neurosci 2002;25:578–588. [PubMed: 12392933]

Stogios PJ, Prive GG. The BACK domain in BTB-kelch proteins. Trends Biochem Sci 2004;29:634–637. [PubMed: 15544948]

Tang CM, Dichter M, Morad M. Quisqualate activates a rapidly inactivating high conductance ionic channel in hippocampal neurons. Science 1989;243:1474–1477. [PubMed: 2467378]

Vignes M, Collingridge GL. The synaptic activation of kainate receptors. Nature 1997;388:179–182. [PubMed: 9217158]

Wang LY, Taverna FA, Huang XP, MacDonald JF, Hampson DR. Phosphorylation and modulation of a kainate receptor (GluR6) by cAMP-dependent protein kinase. Science 1993;259:1173–1175. [PubMed: 8382377]

Wilding TJ, Huettner JE. Activation and desensitization of hippocampal kainate receptors. J Neurosci 1997;17:2713–2721. [PubMed: 9092592]

Wilding TJ, Huettner JE. Functional diversity and developmental changes in rat neuronal kainate receptors. J Physiol 2001;532:411–421. [PubMed: 11306660]

Wisden W, Seeburg PH. A complex mosaic of high–affinity kainate receptors in rat brain. J Neurosci 1993;13:3582–3598. [PubMed: 8393486]

Yan S, Sanders JM, Xu J, Zhu Y, Contractor A, Swanson GT. A C-terminal determinant of GluR6 kainate receptor trafficking. J Neurosci 2004;24:679–691. [PubMed: 14736854]

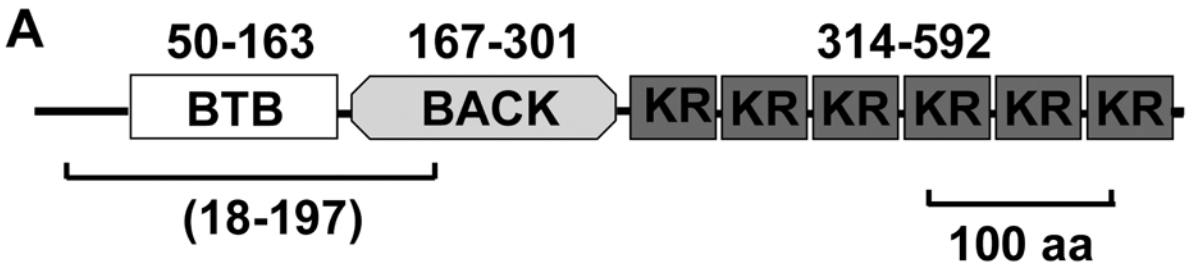


B

| Glutamate receptor C-terminus | KRIP6 (18-197) |
|---|---|
| GluR6a (full length) | +++ |
| $GluR5_{2b}$ (full length) | - |
| GluR7a (full length) | - |
| GluR1 (full length) | - |
| GluR2 (last 50 aa) | - |
| GluR3 (last 50 aa) | - |
| NR2A (last 200 aa) | - |

C

| GluR6 C-terminal region | KRIP6 |
|---|---|
| GluR6 (842-909) | +++ |
| GluR6 (842-899) | +++ |
| GluR6 (842-889) | - |
| GluR6 (842-879) | - |
| GluR6 (842-869) | - |
| GluR6 (890-909) | - |
| GluR6 (879-909) | - |
| GluR6 (871-909) | - |

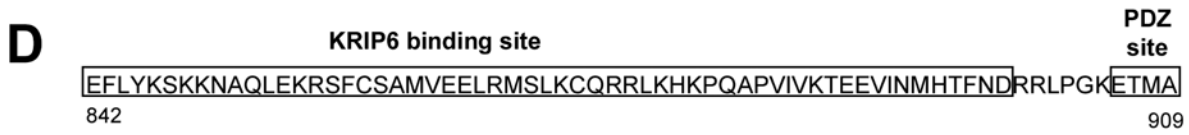


**Figure 1. KRIP6 is a BTB/kelch protein binding to the GluR6a C-terminal domain**

(**A**) The predicted structure of KRIP6 (Kainate Receptor Interacting Protein for GluR6) is shown. KRIP6 has a predicted BTB/POZ domain (50–163), a BACK domain (167–301) and six consecutive kelch repeats (KR; 314–592). Underlined is the fragment isolated from the yeast-two hybrid screen using the GluR6a C-terminal domain as bait. (**B**)Yeast-two hybrid assays showed specific binding of KRIP6 (18-197) with the GluR6a C-terminal domain, but not the C-termini of other glutamate receptors. '+++' indicates growth on histidine and adenine plus strong β-galactosidase activity; '–' indicates lack of growth on histidine or adenine. (**C**) Yeast-two hybrid assay results of GluR6a C-terminal domain truncation mutants with KRIP6 (18-197) are summarized. (**D**) As determined in panel C, the KRIP6 binding region is distinct from the known PDZ-binding domain of GluR6a.

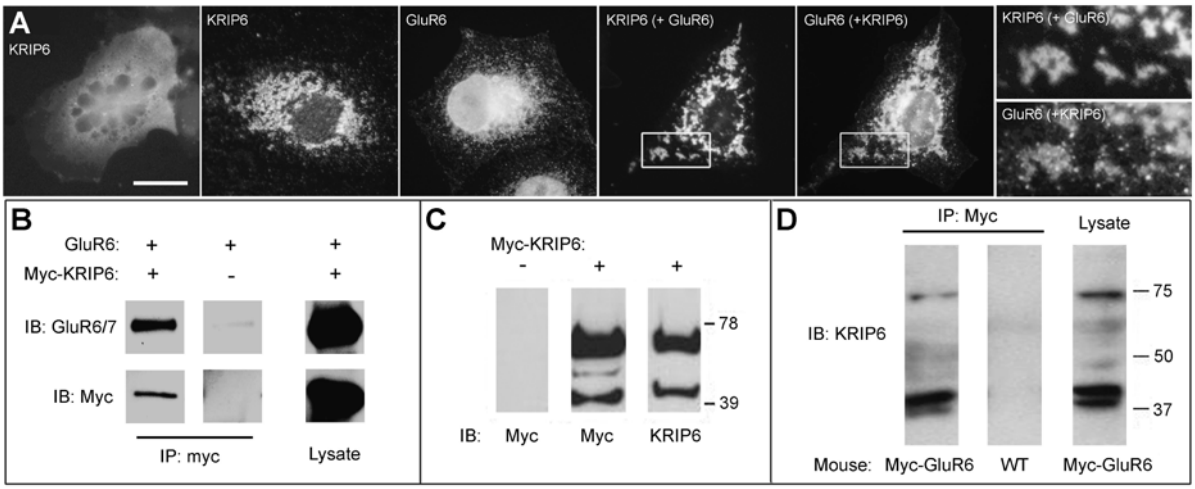


**Figure 2. KRIP6 interacts with GluR6 in COS-7 cells and in brain**

(**A**) CFP-KRIP6 expressed alone in COS-7 cells was either diffusely distributed (far left) or present in clusters (next panel), whereas GluR6 had a different distribution typical of Golgi and plasma membrane localization (third panel from left). Co-expression of CFP-KRIP6 and GluR6 resulted in colocalization in clusters (see inset at high magnification), corresponding to a redistribution of GluR6. Scale bar = 20 μm. (**B**)Immunoprecipitation with myc antibody resulted in co-immunoprecipitation of GluR6 from lysates of COS-7 cells coexpressing myc-KRIP6 but not from cells expressing GluR6 alone. The lysates represent 2.5 % of the material used for immunoprecipitation. Note that the six panels displayed come from the same gel.( **C**) Affinity purified anti-KRIP6 antibody recognizes myc-KRIP6 expressed in COS-7 cells. Two bands, absent in non-transfected COS cells, are observed by Western blot using anti-myc or anti-KRIP6. (**D**) Immunoprecipitation with myc antibody resulted in co-immunoprecipitation of GluR6 from brain lysates of myc-GluR6 transgenic mice but not wild type mice. The lysate represents 2 % of the material used for immunoprecipitation. Thus KRIP6 is present in a complex with GluR6 in brain.

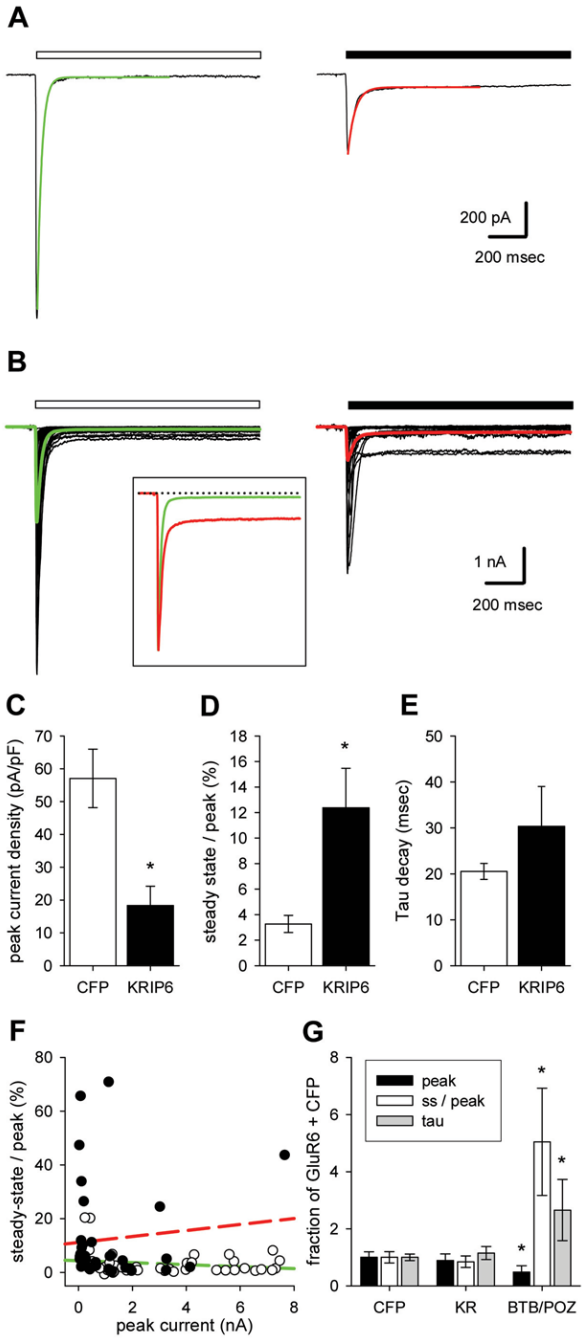


**Figure 3. KRIP6 regulates GluR6-mediated currents in COS-7 cells**

(**A**) Whole-cell currents evoked by 300 μM kainate in COS-7 cells transfected with GluR6 and CFP alone (left) or with CFP-KRIP6 (right). Smooth curves show the best fit of a single exponential decay. Bars above each trace indicate the period of agonist exposure. (**B**) Families of currents recorded in 36 cells transfected with GluR6 and CFP alone (left) and 34 cells transfected with GluR6 and CFP-KRIP6 (right). Superimposed smooth curves show the average of currents evoked in all cells tested. *Inset*: average traces were normalized to the same peak level to illustrate the larger relative amplitude of steady-state current in cells expressing KRIP6. Plots of peak current density (**C**), steady-state current as a percentage of peak current (**D**), and exponential decay time constant, Tau (**E**), and peak current density in cells transfected

with CFP alone (n = 44 cells) or CFP-KRIP6 (KRIP6, n = 35 cells). (**F**) Linear regression of the steady-state/peak ratio versus the peak current amplitude (correlation coefficients = 0.096 for CFP-KRIP6, red line; −0.203for CFP alone, green line). (**G**) For cells transfected with CFP alone, with CFP-KRIP6 (314–600) including the kelch repeats (KR), or with CFP-KRIP6 (1–197) including the BTB/POZ domain (BTB/POZ), plots of peak current density, steady-state/peak ratio and Tau as a fraction of the mean values obtained with CFP alone. (* $p<0.05$).

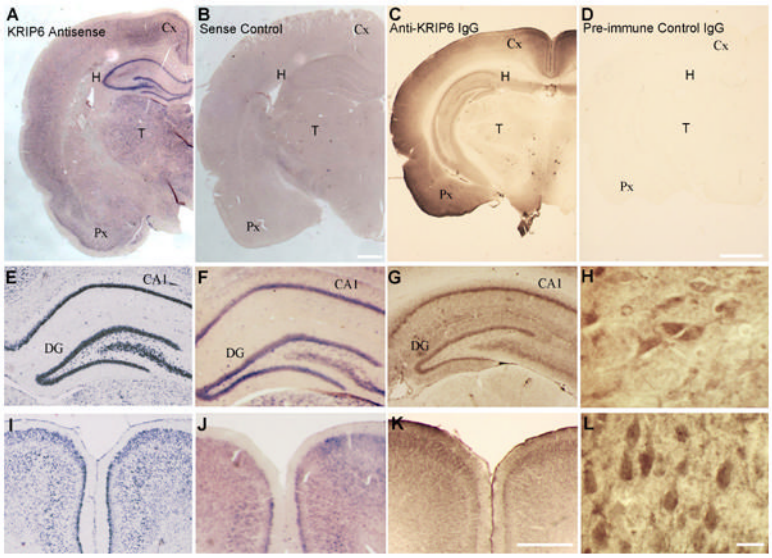


**Figure 4. KRIP6 mRNA and protein are widely expressed in brain**

(**A, B**) In situ hybridization for KRIP6 mRNA on coronal sections of 3 week old rat brain is shown. Antisense riboprobe and sense control probes were used as indicated. (**C**–**D**) Immunostaining of rat brain coronal sections from 3 week old animals using anti-KRIP6 affinity purified IgG (**C**) or pre-immune control IgG (**D**) is shown. KRIP6 mRNA and immunoreactivity are high in cerebral cortex (Cx), piriform cortex (Px) and hippocampus (H); T=Thalamus. (**E**–**L**) Higher magnification images are shown for regions of the hippocampus (**E**–**H**) and cortex (**I**–**L**); DG=Dentate Gyrus. In situ hybridization for KRIP6 mRNA (**F, I**) matches Nissl staining of adjacent sections (**E, J**). Immunoreactivity for KRIP6 in hippocampus (**G, H** hilus) and cortex (**K, L**) indicate concentration of the protein in somata and proximal processes. Scale bars: = 500 μm (**A, B**), 500 μm (**C, D**), 200 μm (**E**–**G, I**–**K**), 20 μm (**H, L**).

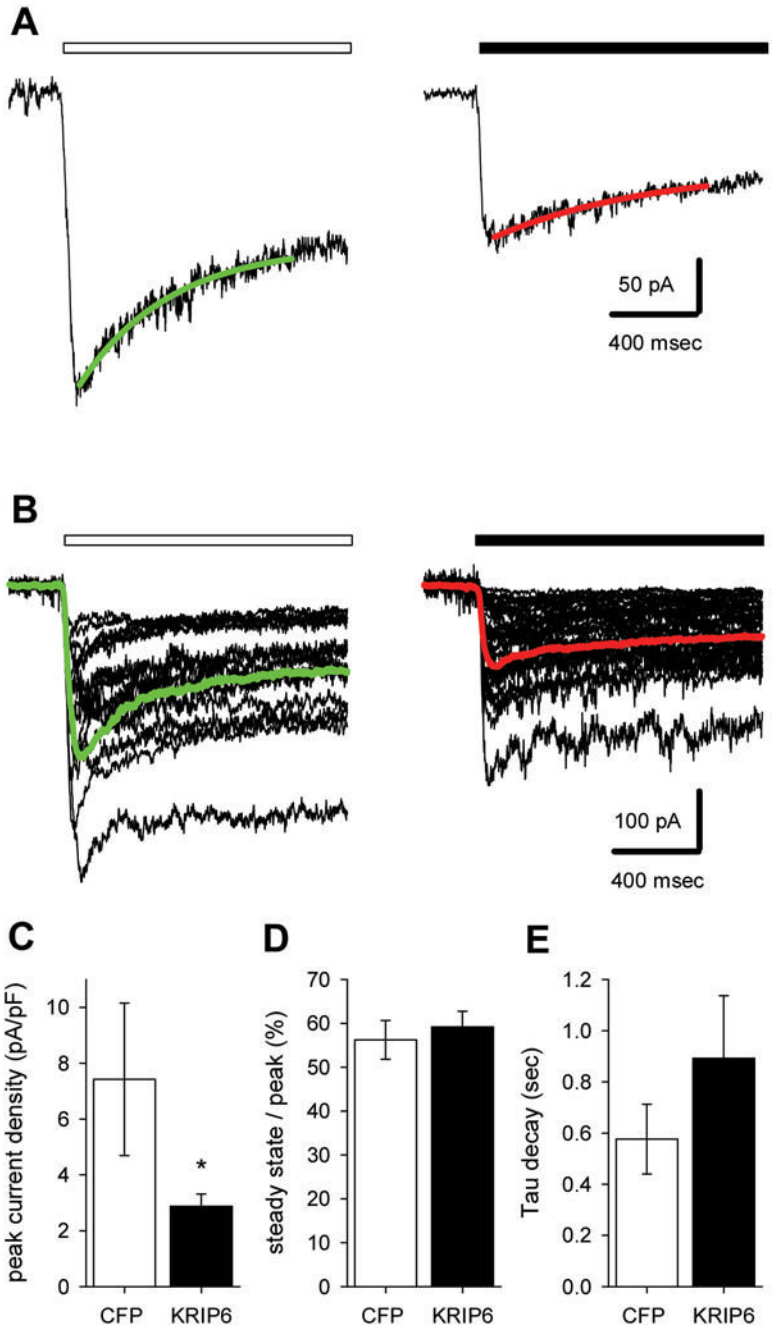


**Figure 5. Overexpression of KRIP6 decreases peak current density of native kainate receptors in hippocampal neurons**

(**A**) Whole-cell currents evoked by 300 μM kainate in hippocampal neurons transfected with CFP alone (left) or with CFP-KRIP6 (right). Smooth curves show the best fit of a single exponential decay. (**B**) Families of currents recorded in 15 cells transfected with CFP alone (left) and 32 cells transfected with CFP-KRIP6 (right). Superimposed smooth curves show the average of currents evoked in all cells tested. Plots of peak current density (**C**), steady-state current as a percentage of peak current (**D**) and exponential decay time constant, Tau (**E**) in neurons transfected with CFP alone (n = 19 cells) or CFP-KRIP6 (n = 42 cells).

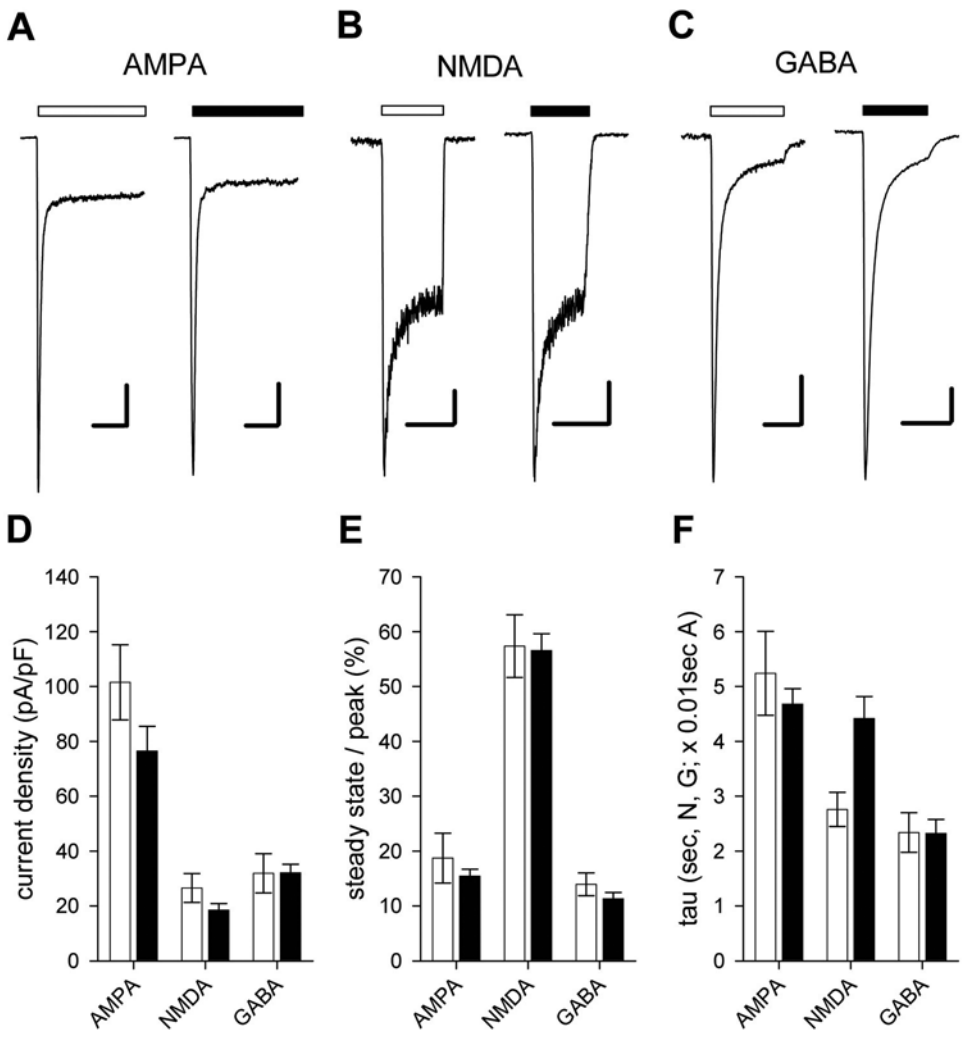


**Figure 6. KRIP6 acts selectively on kainate receptors**

Whole-cell currents evoked by 250 μM AMPA (**A**), 100 μM NMDA, with 1 μM glycine (**B**), or 100 μM GABA (**C**) in hippocampal neurons transfected with CFP alone (open bars indicate the period of agonist exposure), or with CFP-KRIP6 (solid bars). Plots of peak current density (**D**), steady-state current as a percentage of peak current (**E**), and exponential decay time constant, Tau (**F**) in neurons transfected with CFP alone (n = 12–14 cells) or CFP-KRIP6 (n = 18–29 cells). Scales: 500 pA, 0.5 sec (**A**); 100 pA, 20 sec (**B**, CFP), 200 pA, 20 sec (**B**, CFP-KRIP6); 200 pA, 10 sec (**C**).

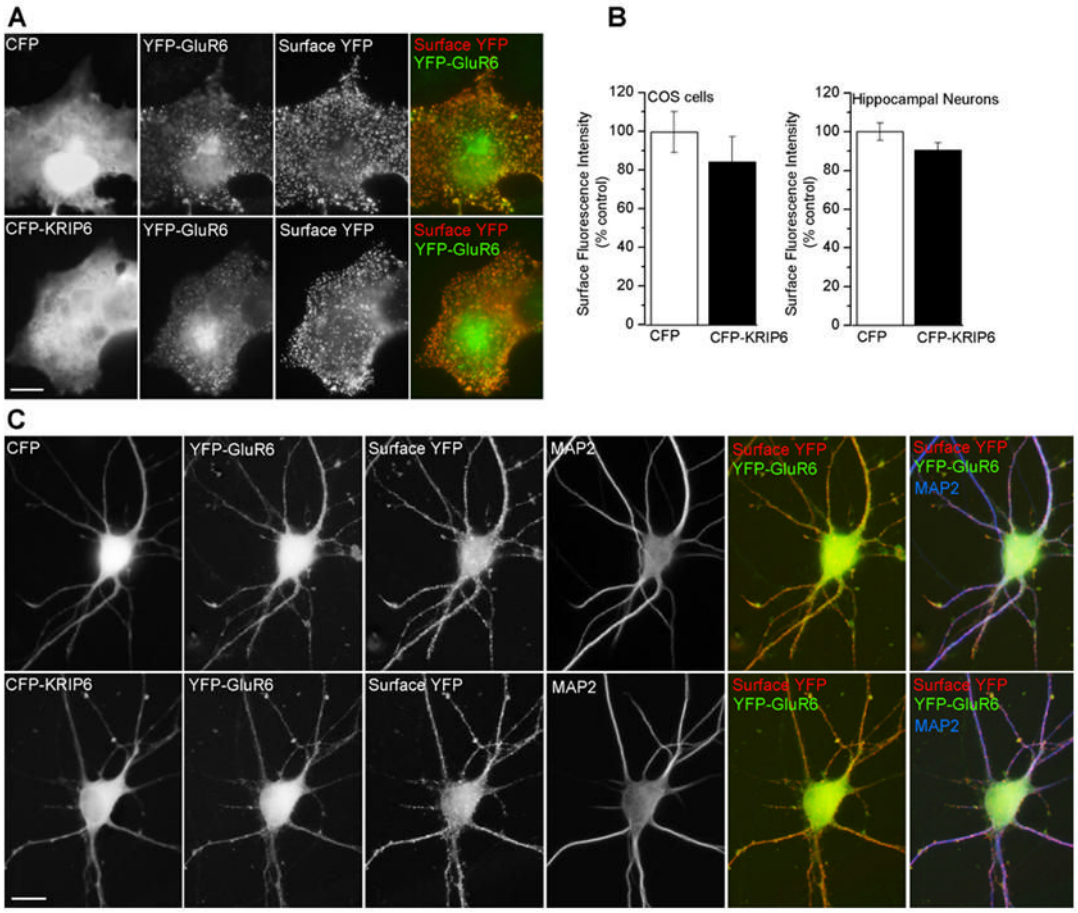


**Figure 7. KRIP6 does not alter surface levels of YFP-GluR6 in COS-7 cells or neurons**

(**A**) Representative examples of COS-7 cells transfected with YFP-GluR6 and CFP or CFP-KRIP6 and immunolabeled live with anti-YFP antibody to reveal surface YFP-GluR6 are shown. (**B**) Absolute surface fluorescence intensity of YFP-GluR6 is unchanged in the presence of CFP-KRIP6 compared to CFP control measured in COS cells or in neurons. (**C**) Surface labeling of YFP-GluR6 in hippocampal neurons transfected together with CFP-KRIP6 or CFP and immunostaining using an anti MAP2 antibody is shown. Surface YFP-GluR6 appears largely somatodendritic and unaffected by coexpression of CFP-KRIP6. Scale bars: 10 μm.